# $M$-band filter banks and dual-tree wavelets for engine combustion and geophysical image analysis

Laurent Duval[a], Caroline Chaux[b] and Jean-Christophe Pesquet[b]

[a]Institut Français du Pétrole, Technology, Computer Science and Applied Mathematics Division, 92500 Rueil-Malmaison, France

[b]Institut Gaspard Monge and UMR-CNRS 8049, Université de Marne-la-Vallée, Champs-sur-Marne 77454 Marne-la-Vallée, France

## ABSTRACT

Signals and images in industrial applications are often subject to strong disturbances and thus require robust methods for their analysis. Since these data are often non-stationary, time-scale or time-frequency tools have demonstrated effectiveness in their handling. More specifically, wavelet transforms and other filter bank generalizations are particularly suitable, due to their discrete implementation. We have recently investigated a specific family of filter banks, the $M$-band dual-tree wavelet, which provides state of the art performance for image restoration. It generalizes an Hilbert pair based decomposition structure, first proposed by N. Kingsbury and further investigated by I. Selesnick. In this work, we apply this frame decomposition to the analysis of two examples of signals and images in an industrial context: detection of structures and noises in geophysical images and the comparison of direct and indirect measurements resulting from engine combustion.

**Keywords:** $M$-band wavelets, Hilbert transform, Dual-tree, Image denoising, Direction analysis.

## 1. INTRODUCTION

Digital signals and images require efficient tools for their analysis. In industrial applications, they are often corrupted by noises, errors or disturbances from different sources, and some attention has to be paid to the use of robust methods. The latters should take also into account classical properties of the data, for instance their non-stationarity. As a consequence, time-scale or time-frequency tools have proven to be particularly useful for these tasks. Amongst these tools, the standard discrete wavelet transform (DWT) has been shown to be very effective both in theory and practice[1] in the processing of certain types of signals, for instance piecewise smooth signals, having a finite number of discontinuities. The DWT implements a form of multiscale analysis, based on successive average/detail type approximations of data. Its most traditional structure relies on a critically sampled or decimated 2-channel filter bank with perfect reconstruction. This decimated structure is particularly efficient for coding applications; for instance in the ongoing standardization of the JPEG 2000 format for image compression. Meanwhile, other processing applications such as data analysis, denoising, detection or restoration often require improvements over the DWT, to overcome its limitations.

Further author information: (Send correspondence to Laurent Duval)
Laurent Duval: E-mail: laurent.duval@ifp.fr, Telephone: +33 (0)1 47 52 61 02
Caroline Chaux: E-mail: caroline.chaux@univ-mlv.fr, Telephone: +33 (0)1 60 95 72 88
Jean-Christophe Pesquet: E-mail: pesquet@univ-mlv.fr, Telephone: +33 (0)1 60 95 77 39

One of the most stricking drawbacks of the DWT relates in one dimension (1D) to the time origin of signals: due to the presence of non shift-invariant operators (the down- and up-samplers), integer time-shifted versions of a signal yield wavelet coefficients which are not shifted accordingly, except at power-of-two time-shifts, depending on the number of resolution levels in the transform. After subsequent processing in the wavelet domain, this results in shift-variant artifacts near jumps or edges in signals or images, which are not desirable in real-world applications since time-shifts are not controlled. In 1D, these artifacts can be avoided or limited by suppressing all (see *e.g.*[2,3] and references therein) or part of the decimators in the transform. As a large majority of proposed solutions to that drawback, limited decimation results in an increased redundancy of the overall transform, making the processing computationally intensive. For instance, for signals of length $N$, discrete shift-invariant or stationary wavelets typically cost $O(N \log N)$ instead of $O(N)$ for DWTs. Industrial applications have used this approach, such as the denoising of a feedback signal for a DC motor with low delay.[4] The same artificial behaviour arises in higher dimensions, but the additional expense then often becomes intractable.

A second drawback further limits the DWT and its most natural redundant extension: tensor products of wavelets usually possess poor directionality in dimensions greater than one. In images, the DWT separates easily horizontal and vertical features, but the diagonal ones generally appear intertwined. This effect constrains the DWT sensitivity in image denoising or feature extraction. Several approaches to overcome this limitation have been developed in the last years, most of them involving a combination of redundancy and improved directionality; for instance: other wavelet frames,[5] bandelets,[6] curvelets,[7] directionlets,[8] as well as other "geometrical" wavelets... Some of these approaches bear a relative amount of complexity. A less expensive design resorts to the union and adequate combination of two traditional wavelet bases: the *dual-tree* discrete wavelet transform, proposed by N. Kingsbury[9] and further addressed by I. Selesnick.[10] It is based on two parallel classical wavelet trees, where corresponding wavelets are approximate reciprocate Hilbert transforms. Combinations of Hilbert and wavelets transforms has been recognized in earlier works[11,12] and rediscovered recently.[13–16]

The third drawback concerns design limitations in two-band decompositions, which heavily constrain the properties of filters. In some applications, it is desirable to use real, orthogonal and symmetric filters with compact supports. The Haar wavelet is the only trivial and somewhat restricted solution in the DWT case. Filter banks with improved properties can be obtained with $M$-band filter banks and wavelets,[17–19] with practical applications.

In recent works, we have investigated the development of a dual-tree $M$-band wavelet decomposition, which reveals a tractable tool for image denoising and restoration. It combines the properties and noise robustness of the 2-band dual-tree wavelet[20] with an increased directional selectivity and reduced aliasing from $M$-band filter banks. This paper aims at presenting two of its industrial applications for the analysis of 1D engine-related signals and 2D geophysical images. The targeted purpose is the extraction of features from signals and images from a very practical standpoint. For more theoretical results including optimal transform construction and extensive results on natural images in simulated noise conditions, we refer to other published material.[21]

The paper is organized as follows. In Section 2 we motivate our work starting from $M$-band filter banks in a general form, with emphasis on uniform design and $M$-band wavelets. We briefly review the construction of the $M$-band dual-tree wavelet transform in Section 3, and also illustrate some of the designed wavelets. Section 4 focuses on two applications: the first one relates to the analysis of seismic images and the separation of features and disturbances into different orientations and frequency bands. The second one addresses the comparison of engine combustion signals coming from direct and indirect measurements, with expensive and low-cost sensors

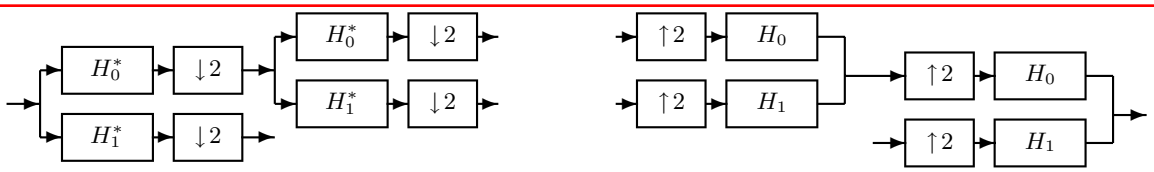


**Figure 1.** Basic two-level discrete wavelet decomposition based on two one-level stages.

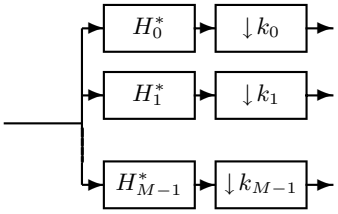


**Figure 2.** General one-level filter bank stage.

respectively. The proposed method is particularly efficient for the analysis of both types of data due to their oscillatory (or directional in 2D) nature. Their relatively low complexity in implementation makes them very appropriate for these applications. Conclusions and perspectives are provided in Section 5.

## 2. GENERAL $M$-BAND FILTER BANKS AND WAVELETS THEORY

### 2.1. Motivations

Traditional discrete dyadic wavelet transforms can be implemented in several ways. The most standard one is akin to the splitting property of the wavelet transform into low- and high-pass components*. Loosely speaking, its building block consists in a low-pass and a high-pass filter associated in parallel, each one followed by a two-fold decimation or downsampling operator, as represented in Fig. 1. The filter coefficients are denoted by the sequences $(h_m[k])_{k\in\mathbb{Z}}$, here with $m \in \{0,1\}$, which are assumed square summable. We will consider that these sequences are real-valued. The Fourier transform of $(h_m[k])_{k\in\mathbb{Z}}$ is a $2\pi$-periodic function, denoted by $H_m$.

From this basic one-level wavelet stage, one can derive the necessary and sufficient conditions for the two filters to satisfy the so-called perfect reconstruction properties. Usually, the wavelet transform results from the iteration of one-level stages following each low-pass branch (as displayed in Fig. 1), which yields the well-known multiscale representation, dividing the frequency axis into dyadic frequency intervals. The practical usefulness of this representation in many data processing tasks is attributed in early works to its relationships with audio or visual perception, and to the wavelet ability to detect singularities, at least in 1D.

The discrete wavelet decomposition has been very successful in several domains, including industrial applications,[22] as illustrated by the adoption of wavelets in the forthcoming compression standard JPEG 2000. Nevertheless, the dyadic structure is not the most appropriate in some cases. Amendments to the DWT, like wavelet packets, add flexibility to the octave decomposition, as demonstrated in the FBI compression standard for fingerprints,[23] which are regarded as medium-frequency images. But due to the relatively tight relationship between the low-pass and the high-pass filters, aliasing distortions may appear when processing both the wavelet or wavelet packets coefficients, *e.g.* in compression or denoising, where some coefficients are cancelled or

*Other implementations include the lifting scheme, Fourier-based algorithms or polyphase representations.

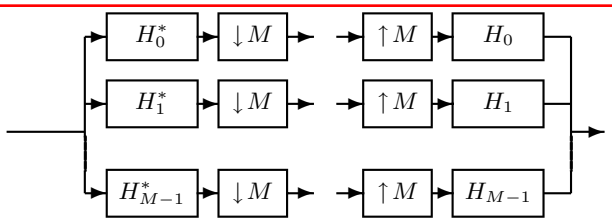


**Figure 3.** General one-level critically sampled $M$-band filter bank stage.

shrinked.[24] A possible solution lies in relaxing some constraints on the one-level wavelet stage depicted in Figure 1 by adding more branches with more filters and modifying the sampling factors. These modifications yield more general multirate systems or filter banks,[25,26] which may comprise several stages of the one-level block depicted in Figure 2, with $M$ branches and arbitrary integer decimation factors $k_m$, $m \in \{0, \ldots, M-1\}$.

This general setting includes usual critically sampled filter banks, as well as oversampled ones,[27,28] which are useful in communications. In many applications, it is more tractable to limit the freedom in the multirate system design. A wealth of results can be obtained by simply using $M$ filters in parallel, with a decimation factor of $M$, *i.e.* $M$-band filter banks (Fig. 3). These filter banks (FBs) yield a rich family of basis functions, including Discrete Cosine/Sine Transforms, Walsh-Paley-Hadamard functions, Malvar's Lapped Orthogonal Transforms[17] (LOTs) and their extensions.[19] With appropriate design, $M$-band FBs, $M > 2$, generally possess sharper frequency than in the dyadic case, resulting in reduced sensitivity to aliasing problems. Moreover, the filters can be orthogonal, symmetric (or anti-symmetric) and real with compact support. Yet, these attractive properties can be enhanced by adding some multiresolution to the overvall transform.[18]

### 2.2. $M$-band wavelets

$M$-band wavelets practically derive from the cascade of $M$-band FBs iterated over the low-pass decimated stage. We focus here on 1D signals belonging to the space $\mathrm{L}^2(\mathbb{R})$ of square integrable functions. An $M$-band multiresolution analysis[18] of $\mathrm{L}^2(\mathbb{R})$ is defined by one scaling function (or father wavelet) $\psi_0 \in \mathrm{L}^2(\mathbb{R})$ and $(M-1)$ mother wavelets $\psi_m \in \mathrm{L}^2(\mathbb{R})$, $m \in \{1, \ldots, M-1\}$. These functions satisfy the following scaling equations:

$$\forall m \in \{0, \ldots, M-1\}, \frac{1}{\sqrt{M}} \psi_m(\frac{t}{M}) = \sum_{k=-\infty}^{\infty} h_m[k] \psi_0(t-k). \tag{1}$$

In the frequency domain, Equation (1) can be re-expressed as:

$$\forall m \in \{0, \ldots, M-1\}, \ \sqrt{M} \widehat{\psi}_m(M\omega) = H_m(\omega) \widehat{\psi}_0(\omega), \tag{2}$$

where $\widehat{a}$ denotes the Fourier transform of a function $a$. For the set of functions $\cup_{m=1}^{M-1} \{M^{-j/2} \psi_m(M^{-j}t - k), (j,k) \in \mathbb{Z}^2\}$ to correspond to an orthonormal basis of $\mathrm{L}^2(\mathbb{R})$, the following para-unitarity conditions must hold:

$$\forall (m, m') \in \{0, \ldots, M-1\}^2, \qquad \sum_{p=0}^{M-1} H_m(\omega + p\frac{2\pi}{M}) H_{m'}^*(\omega + p\frac{2\pi}{M}) = M\delta_{m-m'}, \tag{3}$$

where $\delta_m = 1$ if $m = 0$ and 0 otherwise. The filter with frequency response $H_0$ is associated to a low-pass filter, whereas usually the filter with frequency response $H_m$, $m \in \{1, \ldots, M-2\}$ (resp. $m = M-1$) is band-pass (resp. high-pass). In this case, cascading the $M$-band para-unitary analysis and synthesis FBs, depicted in the upper branch in Fig. 3, allows us to decompose and reconstruct perfectly a given signal.

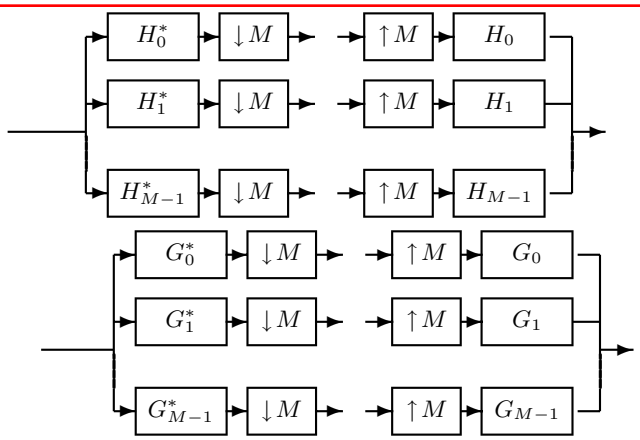


**Figure 4.** A pair of analysis and synthesis $M$-band para-unitary filter banks.

## 3. DUAL-TREE $M$-BAND WAVELETS

### 3.1. Construction of dual-tree $M$-band wavelets

More detail concerning this section can be found in our previous paper.[21] We briefly review the construction of the dual-tree representation. As mentioned before, standard critically decimated $M$-band wavelets are shift-variant. To overcome this difficulty, N. Kingsbury[29] and later I. Selesnick[30] have proposed a dual structure based on two DWT trees whose corresponding wavelets form approximate Hilbert pairs. This implementation is detailed in a tutorial paper[20] by I. Selesnick *et al.*. We present its generalization in the $M$-band form.

A "dual" $M$-band multiresolution analysis is defined by a scaling function $\psi_0^{\mathrm{H}}$ and mother wavelets $\psi_m^{\mathrm{H}}$, $m \in \{1, \ldots, M-1\}$. More precisely, the mother wavelets are obtained by a Hilbert transform from the primal wavelets $\psi_m$, $m \in \{1, \ldots, M-1\}$ defined in Section 2.2. In the Fourier domain, the desired property reads:

$$\forall m \in \{1, \ldots, M-1\}, \qquad \widehat{\psi_m^{\mathrm{H}}}(\omega) = -\imath \, \mathrm{sign}(\omega) \widehat{\psi_m}(\omega), \tag{4}$$

where sign is the signum function defined as:

$$\mathrm{sign}(\omega) = \begin{cases} 1 & \text{if } \omega > 0 \\ 0 & \text{if } \omega = 0 \\ -1 & \text{if } \omega < 0. \end{cases} \tag{5}$$

As it is common in wavelet theory, Equation (4), as well as all equalities in the paper involving square integrable functions, holds almost everywhere. Furthermore, the functions $\psi_m^{\mathrm{H}}$ are defined by scaling equations similar to (1) involving real-valued sequences $(g_m[k])_{k \in \mathbb{Z}}$:

$$\forall m \in \{0, \ldots, M-1\},$$

$$\frac{1}{\sqrt{M}} \psi_m^{\mathrm{H}}\left(\frac{t}{M}\right) = \sum_{k=-\infty}^{\infty} g_m[k] \psi_0^{\mathrm{H}}(t-k) \tag{6}$$

$$\Longleftrightarrow \sqrt{M} \widehat{\psi}_m^{\mathrm{H}}(M\omega) = G_m(\omega) \widehat{\psi}_0^{\mathrm{H}}(\omega). \tag{7}$$

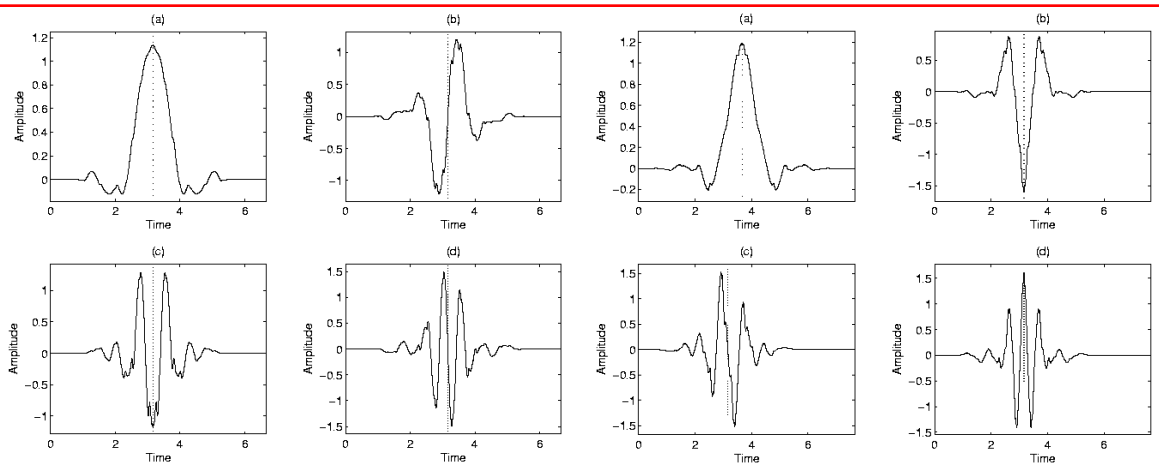


**Figure 5.** One dimensional primal (left) and dual (right) wavelets.

In order to generate a dual $M$-band orthonormal wavelet basis of $\mathrm{L}^2(\mathbb{R})$, the Fourier transforms $G_m$ of the sequences $(g_m[k])_{k\in\mathbb{Z}}$ must also satisfy the para-unitarity conditions:

$$\forall (m,m') \in \{0,\dots,M-1\}^2, \qquad \sum_{p=0}^{M-1} G_m(\omega + p\frac{2\pi}{M}) G^*_{m'}(\omega + p\frac{2\pi}{M}) = M\delta_{m-m'}. \tag{8}$$

The corresponding para-unitary Hilbert FBs are illustrated by the lower branch in Fig. 4.

The Hilbert condition (4) yields

$$\forall m \in \{1,\dots,M-1\}, \qquad |\widehat{\psi}^{\mathrm{H}}_m(\omega)| = |\widehat{\psi}_m(\omega)|. \tag{9}$$

If we further impose that $|\widehat{\psi}^{\mathrm{H}}_0(\omega)| = |\widehat{\psi}_0(\omega)|$, the scaling equations (2) and (7) lead to

$$\forall m \in \{0,\dots,M-1\}, \qquad G_m(\omega) = e^{-\imath\theta_m(\omega)} H_m(\omega), \tag{10}$$

where $\theta_m$ is $2\pi$-periodic. The choice of the phase functions is detailed elsewhere.[21] Figure 5 represents the resulting primal and dual wavelets for a 4-band filter bank[31] in 1D. A linear combination of the two trees results in the 2D wavelets displayed in Figure 6. The following section details the resulting analysis of two types of real-world noisy data. Extensive results on noise-free data are also provided in a preceding work.[21]

## 4. APPLICATIONS

### 4.1. Application to geophysical image analysis

The complexity of seismic data still challenge signal processing algorithms in several applications. If we focus on signal processing, one of the most interesting methods arising from geophysical problems is the wavelet transform, first proposed by J. Morlet *et al.* in the 1980s. Wavelets have finally proven successful for about 10 years in several areas of geosciences, including denoising, deconvolution or migration. Meanwhile, new tools generalizing wavelets have been developed in other research or engineering fields, especially in signal or image processing. Such tools may be useful in geosciences, provided they are adapted to the nature of seismic information. As a recent example of such a transfer, a 2-band dual-tree wavelet was applied to seismic migration.[32] Based on

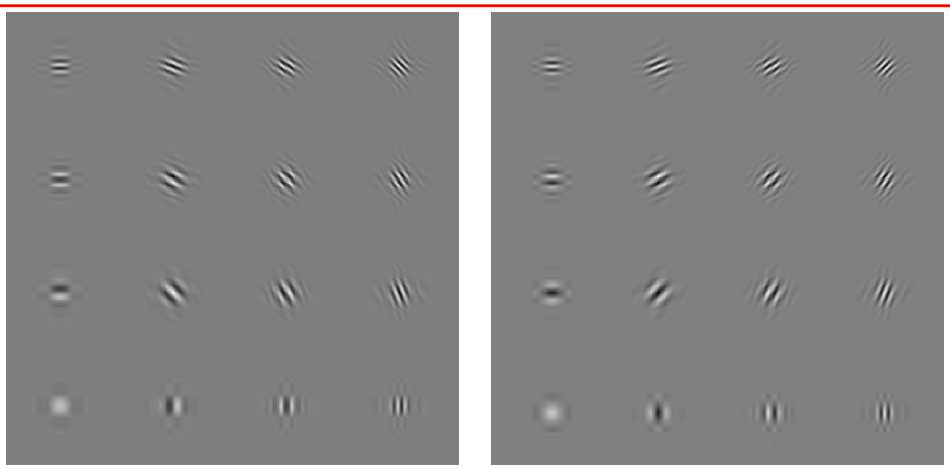

**Figure 6.** Two dimensional primal (left) and dual (right) wavelets.

experiments and observations on seismic data compression, more general transforms have been considered for seismic data, for instance lapped transforms[33] or multi-channel filter banks. Those transforms generally yield a better representation of seismic data than wavelets, due to their short overlapping oscillatory basis functions. On the other hand, the Hilbert transform and complex representations of seismic signals have proven to be very effective, especially for attribute definition. Figure 7 represents an example of a seismic image obtained from waves reflected on a subsurface structure. The layering represents different geological strata.

Its decomposition with a 4-channel dual-tree filter bank is represented in Fig. 8, top and bottom for both orientations. For each orientation, the top-left subimage is the low-pass projection of the decomposition. Horizontally oriented features are represented from top to bottom with increasing frequencies, and vertically oriented features accordingly from left to right.

From its decomposition with a 4-channel dual-tree filter bank (Fig. 8 top and bottom for both orientations), oriented patterns due to processing artifacts can be observed on specific subbands (for instance on the third row, third column of the top subimage). Fine scale information on apparently hidden structures is also apparent from the bottom left of the fourth row, fourth column of the bottom subimage. Since these data are already corrupted by noise, filtering in subbands should be partly supervised.

### 4.2. Application to engine combustion signals

For engine applications, it becomes crucial to detect combustion information in the cylinder to optimize working conditions with respect to consumption and emission reduction. A typical engine block is depicted on Fig. 9-left. Combustion information can be retrieved by using instrumentation in-cylinder pressure sensors. Nevertheless, their price and the environment hostility limit their practical use outside engine test beds. A typical pressure signal (tapered with a raised-cosine window) is represented in solid black on Fig. 9-right. A more cost effective approach consists in using accelerometers located on the engine surface. The engine vibration signal is represented in dotted red on Fig. 9-right. Its vibratory nature is related to the transmission of the fast pressure variations in the cylinder through the engine block. It exhibits non-stationary features due to different kind of disturbances. Transient waves generated by these sources often overlap and the challenge is to detect the components of the vibration signal associated to the combustion only. In this application, we aim at extracting band-pass envelopes

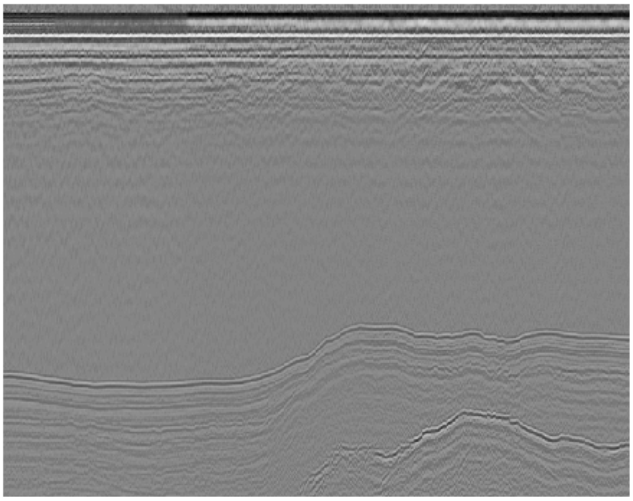

**Figure 7.** Geophysical stack image.

of both signals to match their common behaviour, which is not directly apparent from the signals themselves. Figure 10 represents a simple 2-channel dual-tree wavelet packet decomposition. This decomposition merely iterates the primal and dual FBs. The top row represents the magnitude of both pressure and vibration signals. Each successive row depicts the envelope calculated from the cumulated energy of the subbands in the primal and the dual tree. While the second row does not exhibit an apparent match between the envelopes, the second subimage on the third row seems to display common magnitude trends in both signals, as well as some similar peaks positions in the envelope. This agreement is further refined on the fourth subimage in the last row: for the first samples at least (which correspond to a band-pass subsampled version of the signal envelope), we find a good match between the peak locations in both signals, indicating closely related energy releases for both phenomena. In this application, the approximate shift-invariance of the transform, as well as its noise robustness, are particularly interesting.

## 5. CONCLUSIONS

$M$-band dual-tree wavelets have recently enriched the panel of signal and image analysis methods. They yield improved performance in image filtering and restoration over the DWT and dyadic dual-tree wavelets. They are suitable to industrial contexts due to their relatively low complexity and their robustness to noises. Their application to geophysical image analysis and engine combustion signals is promising for feature extraction and change detection. The authors would like to thank the conference chairs for inviting this communication and Andry Rakotoarimanana for the implementation of the dual-tree wavelet packets.

## REFERENCES

1. S. Mallat, *A wavelet tour of signal processing*, Academic Press, San Diego, USA, 1998.

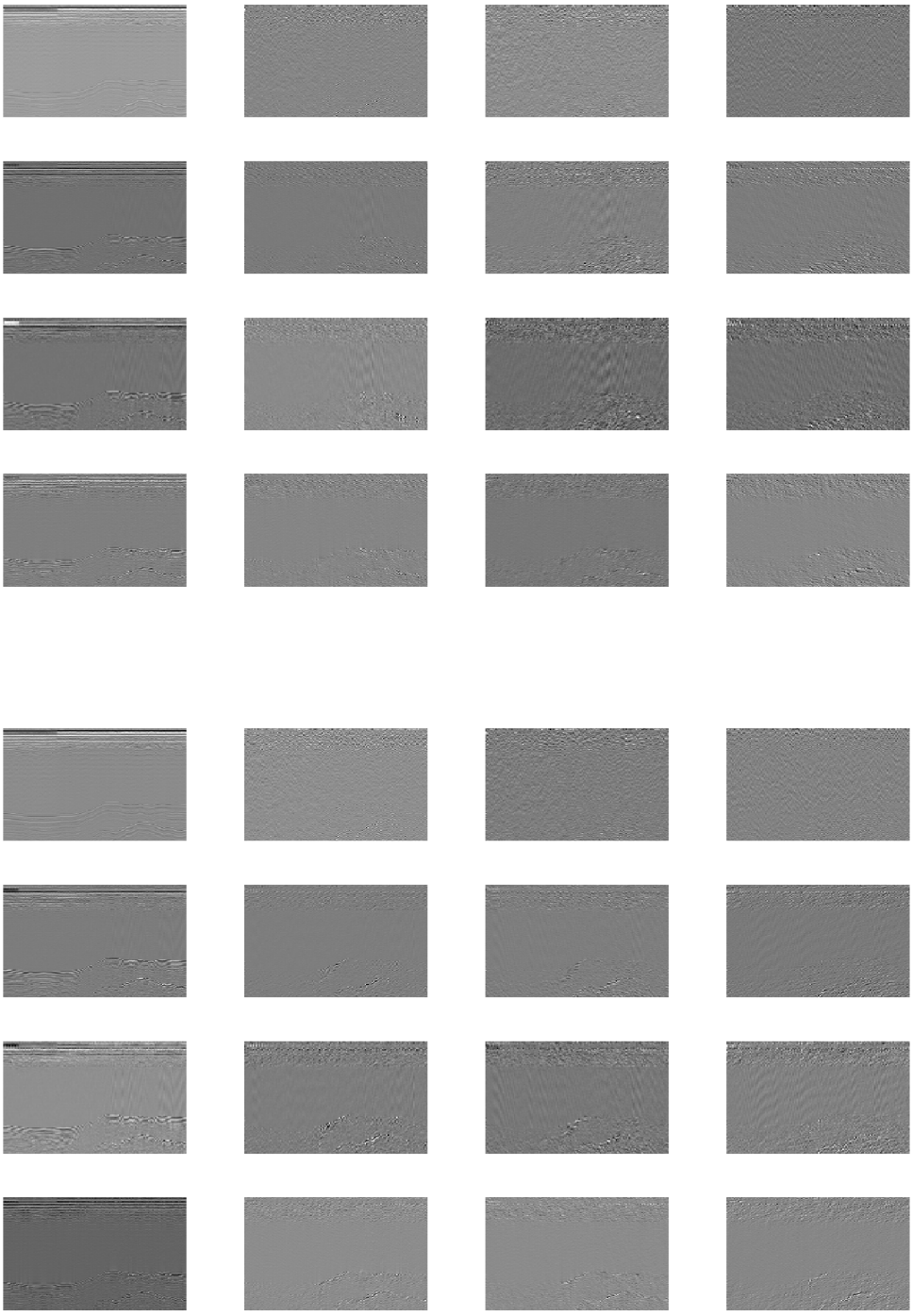

**Figure 8.** Example of a 4-band dual-tree decomposition for the stack image from Fig. 7, for the primal (top) and the dual tree (bottom).

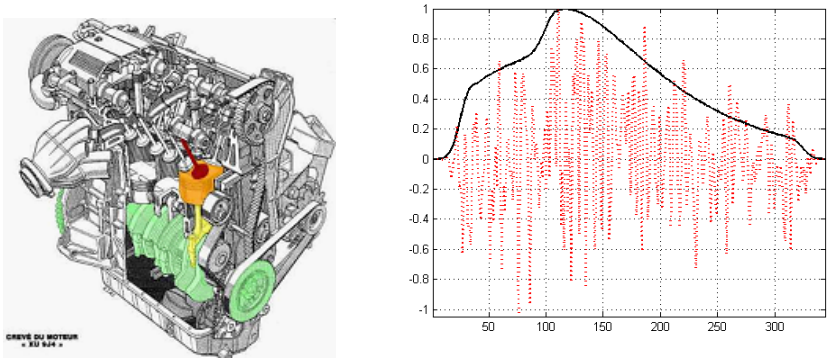

**Figure 9.** Engine block (left) and associated pressure (solid black) and vibration (dotted red) signals.

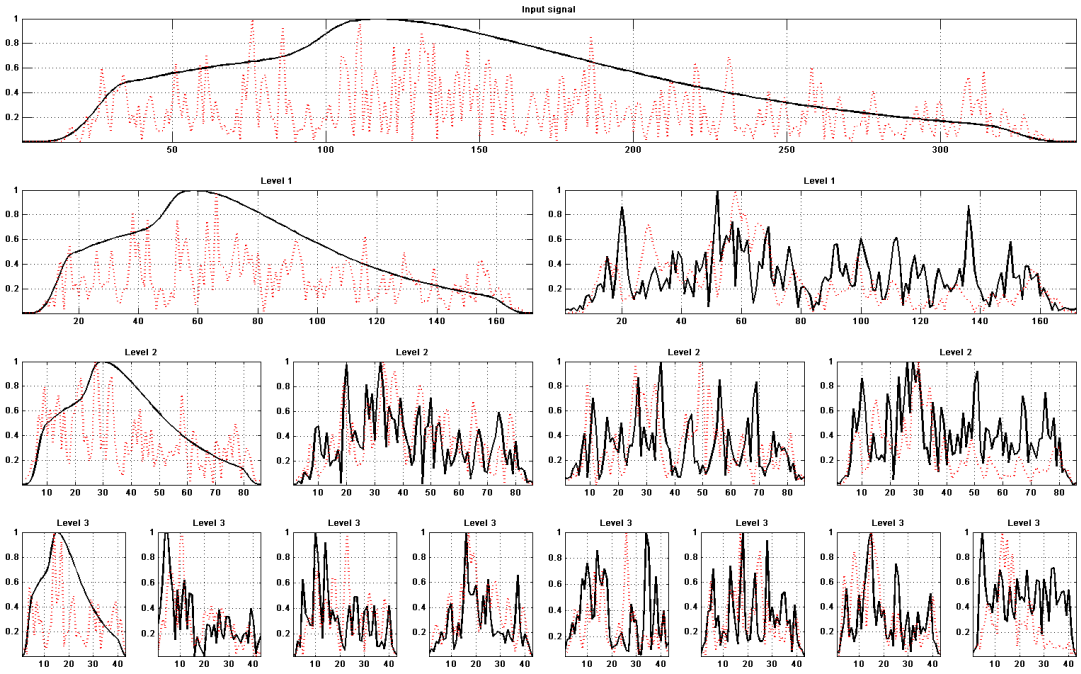


**Figure 10.** A 3-level dual-tree wavelet packet decomposition of a pressure (solid black) and a vibration signal (dotted red) exhibiting envelope correlations at specific levels.

2. G. P. Nason and B. W. Silverman, *Wavelets and Statistics*, vol. 103 of *Lecture Notes in Statistics*, ch. The stationary wavelet transform and some statistical applications, pp. 281–300. Springer-Verlag, New York, NY, USA, 1995.
3. J.-C. Pesquet, H. Krim, and H. Carfatan, "Time-invariant orthogonal wavelet representations," *IEEE Trans. on Signal Proc.* **44**(8), pp. 1964–1970, 1996.
4. P. Tsiotras, D. Jung, and F. Chaplais, "Redundant wavelet filter banks on the half-axis with applications to signal denoising with small delays," *Accepted to Int. J. of Adapt. Control and Signal Processing* , 2006. Preprint.
5. E. Simoncelli and W. T. Freeman, "The steerable pyramid: a flexible architecture for multiscale derivative computation," in *Proc. Int. Conf. on Image Processing*, pp. 444–447, 1995.
6. E. Le Pennec, *Bandelettes et représentation géométrique des images*. PhD thesis, École Polytechnique, France, déc. 2002.
7. E. Candès, L. Demanet, D. Donoho, and L. Ying, "Fast discrete curvelet transforms," *SIAM J. on Mult. Model. Simul.* **5**, pp. 861–899, Mar. 2006.
8. V. Velisavljević, B. Beferull-Lozano, M. Vetterli, and P. L. Dragotti, "Directionlets: anisotropic multidirectional representation with separable filtering," *IEEE Trans. on Image Proc.* **15**, pp. 1916–1933, Jul. 2006.
9. N. G. Kingsbury, "Complex wavelets for shift invariant analysis and filtering of signals," *J. of Appl. and Comp. Harm. Analysis* **10**, pp. 234–253, May 2001.
10. I. W. Selesnick, "Hilbert transform pairs of wavelet bases," *Signal Processing Letters* **8**, pp. 170–173, Jun. 2001.
11. P. Abry and P. Flandrin, "Multiresolution transient detection," in *Proc. Int. Symp. on Time-Freq. and Time-Scale Analysis*, pp. 225–228, (Philadelphia, USA), Oct. 1994.
12. G. Beylkin and B. Torrsani, "Implementation of operators via filter banks: Autocorrelation shell and Hardy wavelets," *Appl. and Comp. Harm. Analysis* **3**, pp. 164–185, 1996.
13. R. van Spaendonck, T. Blu, R. Baraniuk, and M. Vetterli, "Orthogonal Hilbert transform filter banks and wavelets," in *Proc. Int. Conf. on Acoust., Speech and Sig. Proc.*, pp. 505–508, 2003.
14. S. C. Olhede and A. T. Walden, "Analytic wavelet thresholding," *Biometrika* **91**, pp. 955–973, 2004.
15. W. Chan, H. Choi, and R. Baraniuk, "Directional hypercomplex wavelets for multidimensional signal analysis and processing," in *Proc. Int. Conf. on Acoust., Speech and Sig. Proc.*, May 2004.
16. F. Fernandes, M. Wakin, and R. Baraniuk, "Non-redundant, linear-phase, semi-orthogonal, directional complex wavelets," in *Proc. Int. Conf. on Acoust., Speech and Sig. Proc.*, May 2004.
17. H. S. Malvar, *Signal processing with Lapped Transforms*, Artech House, Norward, MA, USA, 1992.
18. P. Steffen, P. N. Heller, R. A. Gopinath, and C. S. Burrus, "Theory of regular $M$-band wavelet bases," *IEEE Trans. on Signal Proc.* **41**, pp. 3497–3511, Dec. 1993.
19. T. D. Tran, R. L. de Queiroz, and T. Q. Nguyen, "Linear phase perfect reconstruction filter bank: lattice structure, design,and application in image coding," *IEEE Trans. on Signal Proc.* **48**, pp. 133–147, Jan. 2000.
20. I. W. Selesnick, R. G. Baraniuk, and N. G. Kingsbury, "The dual-tree complex wavelet transform," *IEEE Signal Processing magazine* , pp. 123–151, 2005.
21. C. Chaux, L. Duval, and J.-C. Pesquet, "Image analysis using a dual-tree $M$-band wavelet transform," *IEEE Trans. on Image Proc.* **15**, pp. 2397–2412, Aug. 2006.

22. F. Truchetet and O. Laligant, "Wavelets in industrial applications: a review," in *Wavelet Applications in Industrial Processing*, **5607**, pp. 1–14, SPIE, (Philadelphie, USA), Oct. 2004.
23. C. B. J. Bradley, R. Onyshczak, and T. Hopper, "The FBI compression standard for digitized fingerprint images," in *Proc. SPIE*, 1996.
24. D. L. Donoho and I. M. Johnstone, "Ideal spatial adaptation by wavelet shrinkage," *Biometrika* **81**, pp. 425–455, Sep. 1994.
25. P. P. Vaidyanathan, *Multirate systems and filter banks*, Prentice Hall, Englewood Cliffs, USA, 1993.
26. G. Strang and T. Nguyen, *Wavelets and Filter Banks*, Wellesley-Cambridge Press, Wellesley, MA, USA, 1996.
27. H. Bölcskei, F. Hlawatsch, and H. Feichtinger, "Frame-theoretic analysis of oversampled filter banks," *IEEE Trans. on Signal Proc.* **46**, pp. 3256–3268, Dec. 1998.
28. V. K. Goyal, J. Kovacevic, and J. Kelner, "Quantized frame expansions with erasures," *Journal of Appl. and Comput. Harmonic Analysis* **10**, pp. 203–233, May 2001.
29. N. G. Kingsbury, "The dual-tree complex wavelet transform: a new technique for shift invariance and directional filters," in *Proc. 8th IEEE Digital Signal Processing Workshop*, (86), 1998.
30. I. W. Selesnick, "Hilbert transform pairs of wavelet bases," *Signal Processing Letters* **8**, pp. 170–173, Jun. 2001.
31. O. Alkin and H. Caglar, "Design of efficient $M$-band coders with linear-phase and perfect-reconstruction properties," *IEEE Trans. on Signal Proc.* **43**(9), pp. 1579–1590, 1995.
32. M. Miller and N. Kingsbury, "Least-square migration using complex wavelets," in *Annual International Meeting*, Soc. of Expl. Geophysicists, (Denver, CO, USA), 2004.
33. L. Duval and T. Røsten, "Filter bank decomposition of seismic data with application to compressionand denoising," in *Annual International Meeting*, pp. 2055–2058, Soc. of Expl. Geophysicists, (Calgary, Canada), 2000.